# PROGRAMMABLE BATCH ASSEMBLY OF MICROPARTS WITH 100% YIELD

*J. Hoo[1*], R. Baskaran[1,2], and K. F. Böhringer[1]*
[1]University of Washington, Seattle, Washington, USA
[2]Intel Corporation, Chandler, Arizona, USA

## ABSTRACT

This paper demonstrates a novel method to perform micropart ($370\times370\times150\mu m^3$) delivery to receptor sites ($20\times10$ array) with a batch assembly process that leads to 100% yield within tens of seconds. The delivery mechanism is statistically characterized and a chemical kinetics inspired model previously proposed is extended. Based on this understanding, repeatable and programmable 100% yield assembly is achieved in open loop and feedback configurations.

## KEYWORDS

Self-assembly, heterogeneous integration, packaging.

## INTRODUCTION

We have previously studied many parallel assembly processes in the microscale as candidates for hetero system integration. These include use of liquid-flow to deliver parts that fall into traps [1], use of surface tension of liquids in predefined locations for part capture including various polymers [2] and solders [3]. We have studied dry (non liquid-flow type) template-based assembly methods in vibratory platforms in the micro scale [4-6]; these assembly methods offer a feasible alternative for materials adverse to fluidic-assembly environments. We also developed a model analogous to chemical kinetics [7] to understand and improve the efficiency and yield of such assembly processes.

Of particular interest to us are assembly applications that require very high packing densities, for instance, the assembly of thermo-electric cooling (TEC) arrays, as well as display-type applications wherein each chip might hold one or multiple pixels.

Batch assembly using vibration is promising as a cost effective and efficient alternative to pick-and-place robots. We propose an assembly methodology that transports and assembles microparts onto a transfer substrate with vibration via an assembly template, and then performs fine-alignment of the assembled parts using capillary forces.

## ASSEMBLY PROCESS FLOW

Our assembly process flow is as shown in Figure 1. It is a refinement over a similar process flow [5] previously presented by our group. In terms of assembly technique, the most significant change is the decision to align and attach our assembly template onto the transfer substrate *before* instead of *after* assembly [5], as shown in Figure 2.
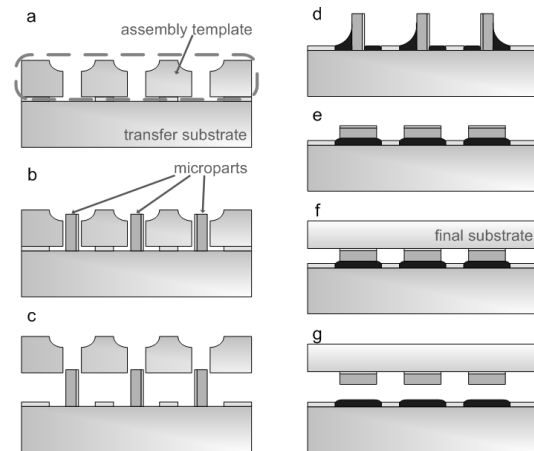


*Figure 1: Full assembly process flow: **a**. mount assembly template on a gold patterned transfer substrate; **b**. assemble parts; **c**. remove template; **d**. apply moisture; **e**. vibrate setup gently to have parts fall on hydrophilic side and self align; **f**. attach parts to destination substrate/device; **g**. complete process by removing assembled substrate/device from transfer template.*
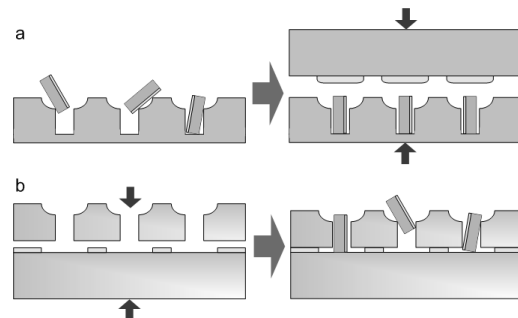


*Figure 2: **a**. alignment of transfer substrate to assembly template is performed after assembly, as proposed in [5]; **b**. assembly template is aligned and attached to transfer template before assembly.*

Modifying our assembly technique from **a** to **b** in Figure 2 allows us to simplify our process flow. In particular, the assembly template and the transfer substrate can be aligned and temporarily bonded together using wafer-wafer alignment tools. It is significantly harder to use said tools to align a transfer substrate onto a template "contaminated" with microparts, and having to then flip the setup over to perform fine alignment by capillary forces and gravity.

Other targeted improvements over the previous iteration includes the ability to handle microparts of smaller dimensions, $370\times370\times150\mu m^3$ from $790\times790\times330\mu m^3$, increasing the maximum possible surface coverage of our technique, 80% from 62% with two assembly passes, and

improving the assembly yield of our methodology. To address the last item, we microfabricated 'funnels' on top of each slot on the assembly template (Figure 1 steps a, b, and c) which effectively increases the "catchment area" of each slot. We also developed a new regime of control for part motion (identified as different modes in Table 1) when we are assembling parts into said slots (Figure 1, step b) that is programmable and can achieve 100% assembly.

*Table 1: Part Movement Modes*

| Mode | Description | Side view |
|------|-------------|-----------|
| Jump-ing | Facilitates directed/random part transport, disassembly of assembled parts and performs initial assembly to be followed-up with walking mode. | |
| Walk-ing | Enables directed part movement without disturbing already assembled parts, permitting 100% assembly, and part removal after assembly. | |
| Station-ary | High-frequency perturbation of parts to prevent effects of stiction between parts and template; the stationary drive regimes do not disturb assembled components. | |
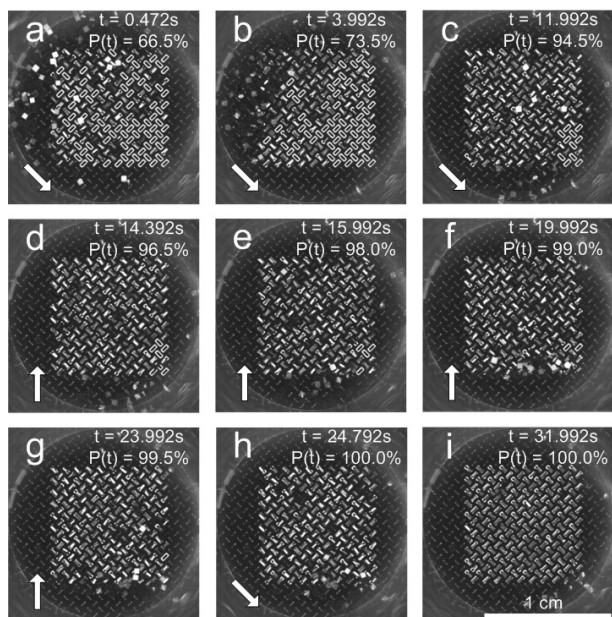


*Figure 3: Various stages of a feedback driven assembly: **a** shows the instance when we switch from jumping mode (with a top-left corner bias) to a walking mode with part-motion direction as indicated by the white arrow in the box. **b**, and **c** show the progressive filling of the entire assembly area. Right after **c**, when assembly-percentage, **P(t)**, has plateaued, we activate a walking mode in the upwards direction as seen in **d, e, f**. and **g**, moving excess parts below the assembly area to the empty sites. After achieving 100% assembly in **h**, we switch to a walking mode towards the lower-right corner, moving excess parts away from the assembly area, finishing the process in **i**; note: size-scale provided in image **i**.*

Using the three movement modes listed in Table 1, we are able to quickly distribute microparts across the entire assembly template using the Jumping Mode. We then move the unassembled parts across the template using the Walking Mode, assembling them into still empty slots, while not risking the disassembly of already assembled microparts. Here, we can employ either feedback (Figure 3) or non-feedback driven methods.

A non-feedback driven method is similar to the sequence shown in Figure 3 except that we walk parts according to a predetermined sequence that, given a certain amount of excess parts, effectively nullifies the possibility that any slot could be left empty after the run. After the completion of either method, parts are walked out of the assembly area as we proceed to Step **c** in Figure 1, where we lift the assembly template from the transfer substrate on which the microparts stand vertically as shown in Figure 4.
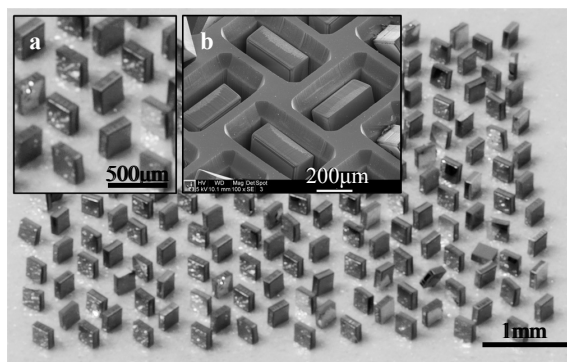


*Figure 4: Parts transferred onto a tape surface after the assembly template has been removed (Figure 1 Step **c**). **a**. shows a zoomed-in view of the standing parts, and **b**. shows parts in slots of the assembly template.*

We have previously shown that by performing the assembly process twice we can double the coverage density of our microparts. A two-pass assembly is a natural fit for TEC array assembly processes where we first assemble p-type microchips in the first pass and n-type in the second, or vice versa.

## FABRICATION AND EXPERIMENTAL SETUP

Our assembly templates are fabricated from silicon wafers using standard microfabricating techniques. The transfer substrates are glass wafers patterned with a gold layer, which is treated with dodecanethiol self-assembled monolayer (SAM) for hydrophobicity. Our test parts are fabricated from SOI wafers, and have one side coated with gold-SAM for side-selectivity.

The assembly template-transfer substrate setup is securely set on a weight-biased platform, which is then set on an electromagnetic vertical actuator (B&K Vibration Exciter Type 4809).
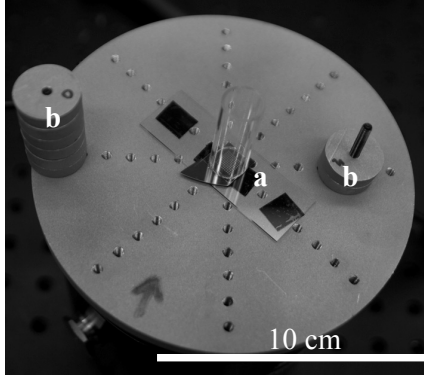
*Figure 5: Weight-biased platform; a. assembly setup; b. weights.*

Figure 5 shows the assembly template-transfer substrate setup in the middle of the platform. A glass tube is mounted onto the assembly setup (also seen in Figure 3) to confine the chips. The platform shown is 6 inches in diameter and will be suitable for larger scaled assembly experiments up to and including 4-inch wafer sized assembly designs.

The distribution of the weights determines the frequencies at which the three micropart movement modes (Table 1) occur, as well as the walking and jumping directions. For example, Table 2 lists the frequencies we used to control the experiment featured in Figure 3.

*Table 2: Specific-case example of part behavior over a range of frequencies. System is calibrated to output 4.65g of vertical actuation at 100Hz.*

| Frequency (Hz) | Mode | Direction |
|---|---|---|
| 100 | Jumping | Random |
| 175 | Jumping | Bottom Right |
| 215 | Jumping | Top Left |
| ~ 300 - 350 | Walking | Top Left |
| ~ 380 - 450 | Walking | Upward |
| ~ 500 - 590 | Walking | Bottom Right |
| > 650 | Stationary | N.A. |

This particular setup provides 4.65g of vertical acceleration at 100Hz, serving as our calibration point. At higher frequencies, this vertical acceleration is coupled into planar acceleration components (due to the biasing weights) that causes the parts to be driven in various planar directions as shown in Table 2; all part motions listed therein are produced by changing only the frequency input to the vertical actuator after the calibration point has been achieved. Higher accelerations increase the speed of part motion in the walking and jumping modes.

Our non-feedback driven assembly process cycles between walking modes of different directions listed in Table 2. By using a suitable number of redundant parts, and predetermining the number of times we need to walk parts

across the assembly area to effectively eliminate the possibility of incomplete assembly, we establish a non-feedback driven assembly process.

Our feedback driven assembly process requires the use of real-time video/image processing feedback to identify the locations of empty slots and thereby direct parts in their direction, as shown in Figure 3.

## RESULTS AND DISCUSSION

When in walking mode with sufficient excess parts, the assembly can be modeled using chemical kinetics analogy as a pseudo first order system, wherein the rate of assembly depends only on the number of unfilled sites. For such a system, the reaction rate constant $k$ is a function of drive frequency and displacement of the sinusoidal drive. Using different input conditions, we experimentally obtain the equivalent rate constants and their distributions by performing analysis on high-speed video recordings of our experiments with custom MATLAB© software. Fixing the voltage/current input to the electromagnetic actuator to put out 4.65g at 100Hz, Figure 6 shows image analysis results from videos of our assembly process on the assembly template shown in Figure 3 with 50% part redundancy at driving frequencies of 525Hz and 565Hz.
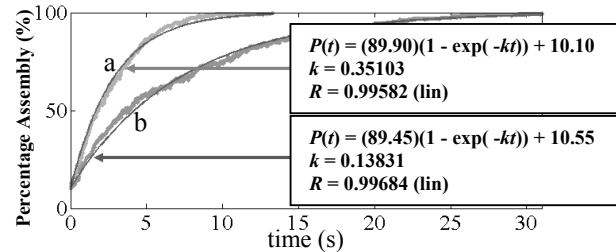


*Figure 6: Image analysis results from two 125 fps videos of our assembly process, driven by a. 525Hz and b. 565Hz, actuator calibrated to output 4.65g at 100Hz, with 50% part redundancy. Our model is fitted into each set of data points to obtain the values for our rate constants k.*

The "quivering" curves in Figure 6, on which our model curves are fitted, are composed of data points of the percentage of assembly of a template (Figure 3) at each 8ms time interval. The constants added into each of the two model equations account for assemblies that have occurred prior to the commencement of our walking mode experiments.

With the exact actuator input parameters and part redundancy as the experiments featured in Figure 6, Figure 7 shows the averages and variances of $k$ for different drive frequencies, derived from 5 experiments per frequency.
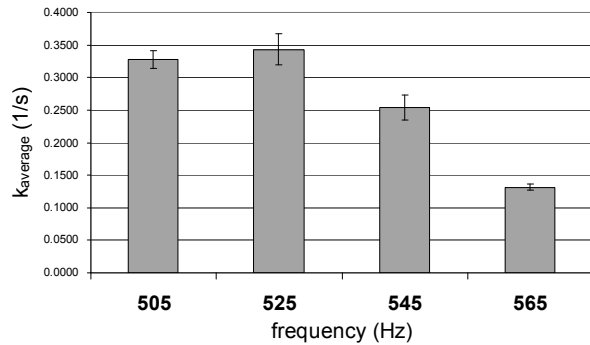
*Figure 7: Averages of rate constant (k) for different drive frequencies, 5 experiments each, at actuator inputs that put out 4.65g at 100Hz vibration, with part redundancy of 50%. Error bars indicates standard deviation.*

The tight distribution of the rate constants shown in Figure 7 is useful for optimization of assembly rates and programmability. Figure 7 also suggests that for this particular experimental configuration, the frequency that exhibits the maximum walking speed, in the direction of interest, is about 525Hz.

Finally, through the course of our experiments, we observe the onset of degradation in our silicon microparts with repeated use. Continuous application of the jumping mode at high accelerations damages the gold layer on one side of our parts, occasionally resulting in peeling. Component damage can be minimized by limiting or excluding the use of the jumping mode. It is conceivable, especially with fragile III-V components, that parts could be introduced on one end of the assembly area and be assembled by walking-only sequences, never applying the jumping mode. Ultimately, component degradation will have to be characterized before actual application of our assembly process.

## CONCLUSION

In summary, we present results of programmable microscale batch assembly leading up to 100% yield with high repeatability. We develop an experimental methodology with automated part counting and assembly rate measurement. We present chemical kinetics based modeling of the assembly process that paves the way for understanding tolerances of assembly to various control parameters and design open loop and feedback enhanced assembly. These advancements in the field of microscale batch assembly bring heterogeneous integration of non-silicon and silicon microelectronics using post fabrication assembly closer to high volume manufacturability, thereby enabling many novel microsystems.

## REFERENCES

[1]     H. J. J. Yeh and J. S. Smith, "Fluidic self-assembly for the integration of GaAs light-emitting diodes on Si substrates," *Photonics Technology Letters, IEEE,* vol. 6, pp. 706-708, 1994.

[2]     R. R. A. Syms, E. M. Yeatman, V. M. Bright, and G. M. Whitesides, "Surface tension-powered self-assembly of microstructures - the state-of-the-art," *Microelectromechanical Systems, Journal of,* vol. 12, pp. 387-417, 2003.

[3]     C. J. Morris and B. A. Parviz, "Micro-scale system integration via molten-alloy driven self-assembly and scaling of metal interconnects," in *Solid-State Sensors, Actuators and Microsystems Conference, 2007. TRANSDUCERS 2007. International*, Piscataway, NJ 08855-1331, United States, 2007, pp. 411-414.

[4]     J. Fang and K. F. Böhringer, "Wafer-level packaging based on uniquely orienting self-assembly (the DUO-SPASS processes)," *Microelectromechanical Systems, Journal of,* vol. 15, pp. 531-540, 2006.

[5]     J. Fang and K. F. Böhringer, "Parallel micro component-to-substrate assembly with controlled poses and high surface coverage," *Journal of Micromechanics and Microengineering,* vol. 16, pp. 721-730, 2006.

[6]     K. Wang, "Template Based High Packing Density Assembly for Microchip Solid State Cooling Application," in *3rd Annual Conference on Foundations of Nanoscience: Selfassembled Architectures and Devices (FNANO)*, Snowbird, 2006.

[7]     R. Baskaran, J. H. Hoo, C. Bowen, and K. F. Böhringer, "Catalyst enhanced micro scale batch assembly," in *Micro Electro Mechanical Systems, 2008. MEMS 2008. IEEE 21st International Conference on*, 2008, pp. 1069-1072.

## CONTACT

* J. Hoo, tel: +1-206-616-6170; jhoo@u.washington.edu